Published in final edited form as:
Exp Cell Res. 2012 August 15; 318(14): 1788–1798. doi:10.1016/j.yexcr.2012.04.022.

CD147 and AGR2 expression promote cellular proliferation and metastasis of Head and Neck Squamous Cell Carcinoma

Larissa Sweeny, MD[a], **Zhiyong Liu, PhD**[a], **Benjamin D. Bush, BS**[a], **Yolanda Hartman, BS**[a], **Tong Zhou**[b], and **Eben L. Rosenthal, MD**[a,*]

[a]University of Alabama at Birmingham, Department of Surgery, Division of Otolaryngology – Head and Neck Surgery, 1670 University Boulevard, Volker Hall G082

[b]Department of Medicine, Division of Immunology and Rheumatology, 1825 University Boulevard, Shelby Biomedical Research Building 302, Birmingham, Alabama, USA

Abstract

The signaling pathways facilitating metastasis of head and neck squamous cell carcinoma (HNSCC) cells are not fully understood. CD147 is a transmembrane glycoprotein known to induce cell migration and invasion. AGR2 is a secreted peptide also known to promote cell metastasis. Here we describe their importance in the migration and invasion of HNSCC cells (FADU and OSC-19) in vitro and in vivo. In vitro, knockdown of CD147 or AGR2 decreased cellular proliferation, migration and invasion. In vivo, knockdown of CD147 or AGR2 expression decreased primary tumor growth as well as regional and distant metastasis.

Keywords

Aerodigestive squamous cell carcinoma; head and neck; metastasis; cd147

Introduction

Head and neck squamous cell carcinoma (HNSCC) is an aggressive malignancy with a propensity for invasion and metastasis. Despite advances in treatment modalities, the prognosis remains poor and survival rates have failed to improve. Contributing to treatment challenges is the underlying complexities of the disease pathogenesis, which remains largely unknown. Furthermore, the ability of HNSCC cells to migrate and invade results in significant regional and distant metastasis and poor patient survival. Limiting the ability of oncogenic cells to regionally and distantly metastasize would improve disease control and outcomes.

In order for an oncogenic cell to migrate and invade, it requires the capability of anchorage-independent growth, the means to break down the components of the extracellular matrix and basement membrane and the ability to promote the formation of new blood vessels [1–

*Corresponding Author: Eben L. Rosenthal, MD, UAB - Division of Otolaryngology, Volker Hall G082, 1670 University Blvd, Birmingham, AL 35233, Tel: (205) 934-9766, Fax: (205) 934-3993, oto@uab.edu.

Conflicts of Interest
The authors have no potential conflicts of interest to disclose.

4]. These requirements can all be facilitated by CD147, also known as extracellular matrix metalloproteinase inducer, a cell membrane bound glycoprotein expressed by several different types of oncogenic cells [5–10]. CD147 allows for oncogenic cells to interact with supporting cells, such as fibroblasts and endothelial cells, resulting in increased expression of matrix metalloproteinases (MMP) and hyaluronan and upregulation of vascular endothelial growth factor [5, 9–11]. As a result, CD147 promotes tumor growth, metastasis and drug resistance [5–7, 12–15].

CD147 is highly expressed in squamous cell carcinomas arising from several anatomical sites, including the head and neck, esophagus, lungs and gastrointestinal track [6, 7, 16–20]. Previous investigations have found high levels of CD147 expression in HNSCC and its expression correlated with tumor progression and lymphatic metastasis [7, 12, 17, 21]. We previously investigated the role of CD147 in HNSCC cell invasion and found CD147 expression by HNSCC cells resulted in increased MMP production by fibroblast and subsequent collagen degradation [8].

The tumor microenvironment also contains the secreted peptide AGR2. Elevation of AGR2 expression has been found in malignancies arising from a variety of anatomical sites, including the esophagus, breast, prostate, pancreas, lung and ovaries [22–30]. Furthermore, AGR2 was found to enhance breast cancer metastasis in xenografts [31]. While the exact function of AGR2 is, for the most part, unknown, it is believed that AGR2 acts as a chaperone, guiding misfolded proteins out of the cell [32, 33]. Several investigations into tumor progression have found AGR2 has a role in promoting cell migration and invasion [22, 23, 31, 34]. To this end we investigated if there was a link between these proteins, CD147 and AGR2, and metastasis of HNSCC cells.

Materials and methods

Clinical tissue specimens

A retrospective review of patients with HNSCC (n=20) was performed following Institutional Review Board approval at the University of Alabama at Birmingham. Tumor histology was confirmed by the pathology department.

Cell lines and tissue culture

Two human HNSCC tumor cell lines were studied: FADU (ATCC; Manassas, VA) and OSC-19 (Jeffrey Myers, The University of Texas M. D. Anderson Cancer Center, Houston, Texas). The cells were obtained, grown, and maintained in Dulbecco's modified Eagle's medium (DMEM) containing 10% fetal bovine serum (FBS) and supplemented penicillin, and streptomycin. The cells were incubated at 37°C in 5% CO_2.

The generation of knockdown CD147 (siE) and AGR2 (siA) HNSCC cell lines has been described previously [35]. Briefly, a short hairpin RNA (shRNA) lentiviral particle delivery system was used to generate CD147-silenced or AGR2-silenced tumor cell lines according to the manufacturer's instructions (Clontech Laboratories Inc., Mountain View, CA). DNA oligonucleotides (listed below) targeting CD147 or AGR2, were separately cloned into pLVX-shRNA1 vector. The vectors with CD147 or AGR2 shRNA were subsequently packaged into lentiviral particles. The lentiviral particles were then transduced into OSC-19 or FADU cells. After selection under puromycin (1 mg/mL), the drug-resistant cells were assessed by flow cytometer for CD147 or AGR2 expression and further confirmed by Western blot. DNA sequences used for knockdown of CD147 or AGR2:

siE1:
GCTGTGAAGTCGTCAGAACATTCAAGAGATGTTCTGACGACTTCACAGTTTTTTG

siE2:
GCAGCACCAGAATGACAAATTCAAGAGATTTGTCATTCTGGTGCTGCTTTTTTG

siA1:
CCGGCAAGACAACAAACCCTTCTCGAGAAGGGTTTGTTGCTTGTCTTGTTTTTTG

siA3:
CCGGCCTTGAGACTTGAAACCAGAACTCGAGTTCTGGTTTCAAGTCTCAAGGTTTTTTG

Reagents

The anti-CD147 antibody was constructed at the University of Alabama at Birmingham (Tong, Z). The antibody is a murine IgG1, protein G affinity- purified, buffered in PBS (pH 7.4) and no preservatives are added. The human AGR2 blocking peptide (Abnova, Taipei City, Taiwan) and supplemental AGR2 peptied (ProSpec Bio, Rehovot, Israel) were purchased commercially.

For imaging regional and distant metastasis panitumumab (Vectibix; Amgen, Thousands Oaks, California), a recombinant, human monoclonal antibody that binds specifically to the extracellular domain of the human EGFR was labeled with IRDye 800CW (IRDye 800CW-*N*-hydroxysuccinimide ester, LI-COR Biosciences, Lincoln, Nebraska). IRDye 800CW is a near-IR fluorescence marker. The labeling process was performed as instructed by the manufacture. Briefly, antibodies were incubated with IRDye 800CW reactive dye in 1M potassium phosphate buffer (pH 9.0) for 1 hour. The unconjugated IRDye 800CW was removed by desalting spin columns (Thermo Fisher Scientific Inc, Rockford, IL). All procedures were conducted under aseptic technique.

In vitro proliferation, migration and invasion assays

To assess the effect of CD147 and AGR2 on cell proliferation, OSC-19 and FADU vector control and knockdown cells (5×10^4) were plated in a 48 well tissue culture treated plate. On day 0 the cells were treated in triplicate with either anti-CD147 monoclonal antibody (0 and 200 μg/mL)[36] or AGR2 blocking peptide at increasing concentrations (0, 10, 100, and 1000 nM; day 0). On day 2 cells were trypsinized and counted with a flow cytometer (Accuri, C6, Ann Arbor, MI).

To determine the role of CD147 and AGR2 on HNSCC migration and invasion, a transwell 2 chamber system was used (Cultrex, Trevigen, Inc., Gaithersburg, MD). The top chamber wells contained porous membranes (8 μm). According to the manufacture's instructions, the top chamber wells were left uncoated (migration) or coated with 0.5X basement membrane extract (BME; 50 μl) overnight (invasion). Cells were serum starved for 24 h, harvested, resuspended in DMEM with 5% FBS (1×10^6/mL) and plated in the top chamber wells (5×10^4 cells/well). Excess liquid in wells coated with BME was aspirated prior to plating. DMEM with 10% FBS was added to the bottom chamber wells (150 μL). Supplemental AGR2 was added to the top and bottom chambers (0, 50 or 200 ng/mL). In additional control chambers, Mitomycin C (10μg/mL) was added to the top well for 2 h to halt proliferation. The chamber system was incubated at 37°C in a CO_2 chamber for 24 h. Each top chamber well was aspirated and the top of the membrane scrapped to remove non-migratory and non-invasive cells. Then bottom side of the membrane was washed with 1X

wash buffer twice and allowed to air dry for 30 min. The membranes were then fixed in methyl alcohol (IMEB Inc., San Marcos, CA) for approximately 60 sec, rinsed with DI water, stained with Azure solution (IMEB Inc., San Marcos, CA) for approximately 60 sec, rinsed with DI water and allowed to dry. Once dry, the underside of the membranes were viewed microscopically. Cells were counted in 2 high power fields (20×) per well.

HNSCC metastatic xenograft mouse model

Athymic female nude mice aged 6 to 8 weeks (Charles River Laboratories and National Cancer Institute–Frederick) were obtained and housed in accordance with our institution's Institutional Animal Care and Use Committee (IACUC) guidelines. To assess role of CD147 and AGR2 in metastasis, an orthotopic tongue tumor model was established by injecting OSC-19 or FADU cells (2.5×10^5) suspended in 30 μL serum-free DMEM into the proximal tongue. Cohorts were divided into vector control, knockdown CD147 or AGR2, or anti-CD147 antibody treatment ($n = 5$ per group). For the treatment cohort, treatment with anti-CD147 (200 μg i.p.) was initiated at the time of tumor cell implantation and administered every 48 h for 2 weeks. Tumors were measured triweekly using calipers to approximate surface area and depth.

Imaging of primary lesions and lymph node metastasis was achieved as previously described [37–39]. The mice were systemically injected with 50 μg of the conjugate 48–72 h prior to being euthanized. At the time of euthanasia, the mice were imaged using the Pearl Impulse (LI-COR Biosciences, Lincoln, Nebraska). The mice were placed in a supine position with arms outstretched and pinned down. A vertical skin incision was made from the rib cage to the lip and the cervical skin was removed. Bright field and fluorescent images of the head and neck were taken pre-dissection, post-dissection and post-excision. Primary tumor and cervical lymph node specimens were collected for pathological analysis.

For the pulmonary metastatic model, nude mice (n=4) were systemically injected with OSC-19 or FADU cell lines, as described previously [40]. Briefly, HNSCC cells (2.5×10^5) were resuspended in 25 μL of DMEM and 175 μL of PBS and injected systemically. Eleven days post-injection, mice were systemically injected with panitumumab-IRDye (50μg). On day 14, mice were sacrificed and the lung harvested. Prior to preparation for histologic processing, the lungs were imaged using the Pearl Imaging System (LI-COR Biosciences, Lincoln, Nebraska).

Histologic analyses

The primary lesions, regional lymph node metastasis and mouse lungs were fixed with 10% formalin solution (Fisher Scientific, Pittsburgh, PA) for one hour, followed by ethanol dehydration after which, tissues were embedded in paraffin wax. Paraffin sections 5 μm thick were stained with hematoxylin and eosin (H&E) for microscopic observation.

Samples were rehydrated in xylene, 95% ethanol, and 70% ethanol. Antigen retrieval was accomplished in 1 mM EDTA, pH 9.0, for 10 min at 100°C. Samples were then allowed to cool at room temperature and blocked with 5% BSA in TBST for 10 mins at room temperature. Then the protocol for either immunohistochemical or immunofluorescence staining was preformed (see below).

Immunohistochemical analysis was performed to determine keratin expression. Primary antibody, pan cytokeratin (Abcam, Cambridge, MA), was applied at the concentrations recommended and allowed to incubate for 1 h. Secondary antibodies (horseradish peroxidase) were applied for 1 h in a humidified chamber at room temperature. DAB substrate was then applied to slides and allowed to incubate at room temperature until

appropriate color developed. Samples were then counterstained with Harris Hematoxylin diluted 1:1 with tap water for 45 sec. Finally, samples were dehydrated and counted with Permount and allowed to dry overnight.

Immunofluorescence analysis was performed to determine expression of CD147 and AGR2. The sections were incubated for one hour at room temperature in a humidified chamber with antibody to both 1:100 CD147 (Millipore, Billerica, MA) and AGR2 (Abcam, Cambridge, MA). Slides were then washed 3 times in 0.05 M Tris-Buffer, pH 7.6 for 10 min. and then incubated in the dark for 1 h using a mixture of fluorophore-linked secondary anti-bodies 1:100 (AlexaFluor 568-conjugated goat anti-mouse IgG1 and AlexaFluor 488-conjugated goat anti-rabbit IgG; Invitrogen, Grand Island, NY). The slides were then washed 3 times in 0.05 M Tris-Buffer, pH 7.6 for 10 min each and mounted using Gel Mount Aqueous Mounting Medium (Sigma, G0918). Fluorescence microscopy was performed for each field using Olympus IX70 fluorescence microscope with Olympus DP72 camera. Images were then processed using Olympus D2-Basic Imaging Software.

Western blot analysis

Cells were grown to 70%–80% confluence, washed twice with cold PBS, and lysed in lysis buffer [50mM Tris-HCl (pH7.5), 150mM NaCl, 1% (v/v) NP40, 0.5 % (w/v) sodium deoxycholate, 1mM EDTA, 0.1% SDS], and a protease inhibitor cocktail tablet (Roche Applied Science, Indianapolis, IN) was added. The cleared lysates were collected by centrifugation at 12000 x g for 20 mins at 40°C. The protein concentrations were measured by BCA protein assay (Thermo Scientific, Rockford, IL). Lysates with 10 μg of total protein were resolved by SDS PAGE and transferred to PVDF membranes. The membranes were incubated with the primary antibody. After washing and incubating with horseradish peroxidase conjugated secondary antibodies, the membranes were washed again and detected by the Amersham ECL Western blotting detection system (GE healthcare, Buckinghamshire, UK). The membranes were reprobed with horseradish peroxidase-conjugated mouse monoclonal antihuman β-actin to ensure equal protein loading.

Gelatin zymography analysis

Tumors were harvested, placed in lysis buffer [50mM Tris-HCl (pH7.5), 150mM NaCl, 1% (v/v) NP40, 0.5 % (w/v) sodium deoxycholate, 1mM EDTA, 0.1% SDS] plus a protease inhibitor cocktail (Roche Applied Science, Indianapolis, IN) and sonicated. The cleared lysates were collected by centrifugation at 12000 x g for 20 mins at 40°C. The protein concentrations were measured by BCA protein assay (Thermo Scientific, Rockford, IL). Each sample (25 μL) was mixed with 2X tris-glycine SDS buffer (25 μL; Novex, Life Technologies) and 40 μL was loaded on Novex 10% zymogram gel (0.1% gelatin, 1.0 mm, 10 well). Electrophoresis was run using SDS running buffer for 1.5 hrs at 125 V. The gel was renatured in zymogram renaturing buffer (100 mL; Novex) with gentle agitation at room temperature for 30 min. The gel was then developed in zymogram developing buffer (Novex) with gentle agitation at 37°C for 12 h. The gel was then washed with DI water three times and incubated with SimplyBlue safe stain (Life Technologies) for 3 days. Clear bands on a uniformly stained background represent areas of gelatinolytic activity. FBS was loaded as control.

Statistical analyses

Data analyses of in vitro cell growth and in vivo xenografts growth were done using GraphPad Prism software (GraphPad Software, Inc., San Diego, CA). Quantitative data was expressed as a mean ± standard error (SE). Equation for volume of an elliptoid [volume = (4/3)(3.14)(length)(width)(depth)] was used to calculate in vivo tongue tumor volume. $p < 0.05$ was considered significant in unpaired *t*-test analysis used to determine differences

between groups. Western blot or zymogram band intensities were quantified using ImageJ (http://rsb.info.nih.gov/ij/) and normalized to beta-actin.

Results

CD147 and AGR2 expression and localization in HNSCC specimens

To evaluate the expression patterns of CD147 and AGR2 in HNSCC, immunofluorescence analysis of clinical tissue specimens was performed. CD147 expression was primarily membranous, while AGR2 immunoreactivity was predominately cytoplasmic (Fig. 1) [23]. Approximately half of the oncogenic cells demonstrated CD147 expression (48.8 ± 7.6 %) while close to a third demonstrated AGR2 immunoreactivity (34.5 ± 6.4 %). Furthermore, consistent with previous findings, CD147 expression was primarily on oncogenic cells near the invading front [10]. Cytoplasmic immunoreactivity of AGR2 correlated with membranous expression of CD147 in all but one specimen (95%, n=19). Of the HNSCC tissue specimens with correlating immunoreactivity patterns, approximately half had greater than 50% of cancer cells with positive staining (47%, n=9).

Differential expression of CD147 and AGR2

Relative protein expression levels on western blot analysis verified knockdown of CD147 (shRNA) decreased CD147 expression by OSC-19/siE1 (77.1%) and FADU/siE2 (61.1%) cell lines relative to vector control (VC). When assessing AGR2 expression, it was found that knockdown of CD147 also resulted in an absence of AGR2 expression. However, knockdown of AGR2 (siA) only slightly decreased CD147 expression by OSC-19/siA1 (86.4%) and increased CD147 expression by OSC-19/siA3 (155%). Additionally, knockdown of AGR2 did not effect CD147 expression by FADU/siA1 (96.5%) and FADU/siA3 (94.1%) (Fig. 2).

Inhibition or knockdown of CD147 or AGR2 expression decreases HNSCC cell proliferation in vitro

To determine the effect of CD147 and AGR2 expression on HNSCC cell proliferation, OSC-19 and FADU vector control and knockdown (siE1 or siE2, siA1, siA3) cell lines were seeded in triplicate, grown for 48 h and counted by a flow cytometer. Relative to vector control, a reduction of CD147 or AGR2 expression resulted in a significant decrease in cell proliferation ($p < 0.0001$). Similarly, treatment with the anti-CD147 monoclonal antibody significantly decreased proliferation of OSC-19/VC and FADU/VC cells ($p < 0.0001$). However, treatment had no effect on proliferation of the knockdown AGR2 cell lines (Fig. 2B).

To determine if blocking AGR2 reduced proliferation of HNSCC cells, OSC-19/VC and FADU/VC cells were seeded in triplicate and incubated with an AGR2 blocking peptide (0–1000 nM) for 48 h. Treatment significantly decreased OSC-19/VC cell proliferation at all concentrations ($p < 0.001$) and significantly decreased FADU/VC cell proliferation at 100 ($p < 0.05$) and 1000 nM ($p < 0.001$) concentrations (Fig. 2C). However, similar inhibition of cells with knockdown CD147 or AGR2 expression did not significantly decrease proliferation further (data not shown).

CD147 and AGR2 effect HNSCC migration and invasion

Migration (no BME) and invasion (BME coated) were evaluated by a transwell chamber system. The BME contained several of the components found in the basement membrane (laminin, collagen IV, entactin, heparin sulfate proteoglycan) and subsequently served as a basement membrane model. Reduction in CD147 or AGR2 expression significantly

decreased both migration and invasion of OSC-19 and FADU knockdown cells compared to vector control ($p < 0.001$; Fig. 3A). Addition of AGR2 to the media did not affect migration and invasion of OSC-19/VC or FADU/VC cell lines. However, supplementing the media with either 50 or 200 ng/mL of AGR2 significantly increased both invasion and migration of both the OSC-19 and FADU knockdown CD147 and AGR2 cell lines (Fig. 3B–C). This supports the hypothesis that supplemental AGR2 can compensate for the loss of AGR2 or CD147, suggesting a codependence.

Knockdown of CD147 decreased primary tumor growth and reduced the incidence of cervical lymph node metastasis in vivo

The role of CD147 and AGR2 in primary tumor growth and cervical lymph node metastasis was assessed using an oral cavity orthotopic tongue model. OSC-19 or FADU (VC, siE, siA1, siA3) cells were implanted in the proximal tongue of athymic nude mice (n=5/group). To determine the effect of CD147 and AGR2 expression on tumor growth rate, tumor volume was measured beginning on day 4 post-inoculation. By day 8 post-inoculation, the OSC-19/VC had significantly larger mean tumor volumes (240.9 ± 17.8 mm^3) compared to OSC-19/siE1 (58.4 ± 15.0 mm^3; $p < 0.0001$), OSC-19/siA1 (120.3 ± 15.9 mm^3; $p = 0.001$) or OSC-19/siA3 (26.4 ± 9.5 mm^3; $p < 0.0001$). This reduced growth rate was maintained until the conclusion of the study on day 16. The OSC-19/VC continued to have significantly larger tumor volumes (597.4 ± 52.8 mm^3) compared to OSC-19/siE1 (336.0 ± 69.0 mm^3; $p = 0.017$), OSC-19/siA1 (428.4 ± 64.6 mm^3; $p = 0.077$) or OSC-19/siA3 (265.8 ± 83.4 mm^3; $p = 0.0099$)(Fig. 4A). There was a significant reduction in tumor growth rate for the FADU/siE2, FADU/siA1 and FADU/siA3 xenografts compared to FADU/VC. By day 16 post-inoculation, the FADU/VC xenografts had significantly larger tumor volumes (624.2 ± 65.5 mm^2) compared to FADU/siE2 (16.3 ± 12.2 mm^2; $p < 0.0001$), FADU/siA1 (10.1 ± 10.1 mm^2; $p < 0.0001$) or FADU/siA3 (12.6 ± 12.6 mm^2; $p < 0.0001$)(Fig. 4B).

The knockdown FADU cells had such profound reduction in tumor growth, several xenografts had no evidence of disease at the time vector control xenografts required euthanasia. As a result, only the OSC-19 xenografts and regional lymph nodes were resected and processed for histologic analyses. Targeted fluorescence imaging assisted in localization of disease (Fig. 4C). Microscopically, primary lesions and lymph node metastasis were detected by H&E and confirmed by probing with anti-human cytokeratin. Cervical lymph node metastases were detected in all OSC-19 xenografts. However, there was a significant decrease in the mean number of positive lymph nodes found in xenografts inoculated with knockdown cells relative to vector control: OSC-19/VC (5 ± 0.5), OSC-19/siE (3 ± 0.3, $p = 0.029$), OSC-19/siA1 (3 ± 0.4, $p = 0.015$) and OSC-19/siA3 (2 ± 0.3, $p = 0.005$) (Fig. 4D).

Primary lesions underwent further histologic analyses for CD147 and AGR2 expression (Fig. 5). Relative to OSC-19/VC (87 ± 4.4%), there was a significant reduction in CD147 immunoreactivity in OSC-19/siE (30 ± 3.5%, $p < 0.0001$). Consistent with in vitro data, the knockdown of CD147 or AGR2 decreased AGR2 expression in vivo: OSC-19/siE (22 ± 6.0%, $p = 0.0005$), OSC-19/siA1 (11 ± 2.9%, $p < 0.0001$) and OSC-19/siA1 (15 ± 2.2%, $p < 0.0001$) xenografts relative to OSC-19/VC (66 ± 4.9%). This data suggests that AGR2 and CD147 may be co-regulated and influence one another.

Inhibiting CD147 decreased primary tumor growth and reduced incidence of cervical lymph node metastasis in vivo

Orthotopic OSC-19 xenografts were divided into two cohorts: control and anti-CD147 treatment. Treatment (200 μg i.p.) was begun on the day of tumor cell implantation. By day 8, there was a significant reduction in tumor growth rate ($p = 0.003$; Fig. 6A). The reduction in tumor growth continued for the duration of treatment ($p = 00.021$). The incidence of

positive lymph nodes was similar between the two cohorts. However, none of the mice in treatment cohort had evidence of BLN metastasis while 60% (n=3) had positive BLN in the control group (Fig. 6B).

Primary tumor specimens were harvested and lysates prepared for western blot and zymogram analysis (Fig. 6C). There was a trend toward decreased CD147 ($p = 0.32$) and AGR2 ($p = 0.08$) expression in the treatment group. Furthermore, there was a significant decrease in active MMP2 expression ($p = 0.05$) in the treatment cohort. Active MMP9 expression was similar for both cohorts.

Silencing CD147 and AGR2 reduced pulmonary metastasis

To assess the effects of CD147 and AGR2 on the incidence of distant metastasis, OSC-19 and FADU cells were injected systemically into nude mice [40]. On day 14 following injection of the cells, the mouse lungs were harvested. The number of pulmonary metastasis seen on by fluorescence imaging was confirmed by histological analysis. There was trend towards a lower incidence of pulmonary metastasis for OSC-19/siE1 ($p = 0.24$) and OSC-19/siA1 ($p = 0.35$) compared to OSC-19/VC (Supplemental Fig. 1A). There was a significantly lower incidence of pulmonary metastasis for FADU/siE2 ($p = 0.08$) and FADU/siA1 ($p = 0.04$) compared to FADU/VC (Supplemental Fig. 1B).

Discussion

There is limited understanding of the pathogenesis which allows head and neck oncogenic cells to metastasize. Previous investigations by our lab and others, have found CD147 is highly expressed in HNSCC and plays a role in oncogenic cell invasion [6, 8, 10, 12, 15–17, 19, 41, 42]. Furthermore, CD147 expression levels have been found to correlate with progression of disease, prognosis and lymph node metastasis in HNSCC [6, 12, 16]. However, its effect on regional and distant metastasis of HNSCC cells in vivo has not yet been elucidated. Moreover, to our knowledge, the relationship between AGR2 and metastasis of HNSCC has not previously been investigated. This study explored the relationship between CD147 and AGR2 and provides novel data to support the role of AGR2 in the promotion of HNSCC tumorigenesis and metastasis.

It is well known HNSCC cells have a propensity to invade and migrate resulting in a high incidence of regional and distant metastasis, decreasing survival and prognosis. It is becoming increasingly evident that the ability of oncogenic cells to migrate and invade is dependent on a complex set of interactions with components of the tumor microenvironment. CD147, a highly glycosylated transmembrane protein, behaves as a coordinator for oncogenic cell migration and invasion via regulation of essential molecular events necessary for carcinogenesis [10]. Following malignant transformation of a normal cell into an oncogenic cell, CD147 facilitates each phase of oncogenesis. CD147 promotes proliferation, induces VEGF expression and angiogenesis, stimulates proteolytic enzyme expression and enables anchorage-independent growth [5, 9, 12, 41–44]. As a result, oncogenic cells are able to migrate, invade and metastasize [1, 10, 44, 45]. AGR2, a secreted peptide, has also been found to promote growth and metastasis and allow for anchorage-independent growth. Therefore, in tumorigenesis there may be a collaborative relationship between AGR2 and CD147 [22]. In this study, we demonstrated HNSCC cell proliferation, tumor growth rate and metastasis was reduced by a reduction in either CD147 or AGR2 expression.

Both CD147 and AGR2 are believed to increase anchorage-independent growth of oncogenic cells, permitting the cells to migrate and seed a location an appreciable distance from the primary tumor cell population [10, 22, 30, 32, 42]. To study the effects of CD147

and AGR2 on the migration of HNSCC cells, we assessed the ability of HNSCC cells to migrate from the top of a porous membrane to its underside. Relative to vector control cell lines, we found knockdown of CD147 or AGR2 expression decreased the migratory behavior of HNSCC ($p < 0.0001$). Furthermore, addition of AGR2 to the media increased the number of migratory CD147 or AGR2 knockdown cells ($p < 0.05$).

Oncogenic cells create a pericellular environment containing signaling agents necessary to ensure their survival and tumorigenesis. HNSCC cells crosstalk with supporting cells, such as fibroblasts, in the tumor microenvironment to promote MMP expression [8, 46, 47]. CD147 facilitates cell invasion by induction of proteases (MMPs) which degrade and remodel the extracellular matrix [5]. The result is oncogenic cells are able to traverse the basement membrane and extracellular matrix and invade regional and distant tissues. In accordance, CD147 expression has been found to be significantly higher at the invasive front of HNSCC specimens relative to the more differentiated core [10]. Several of the HNSCC specimens in this study demonstrated similar findings, with high CD147 expression by the oncogenic cells located near the invading edge. In order to simulate a basement membrane in vitro, we coated porous membranes with basement membrane extracts containing type IV collagen, laminin, entactin and heparin sulfate proteoglycan. Relative to vector control, knockdown of CD147 and AGR2 significantly reduced the ability of HNSCC cells to invade and traverse the basement membrane ($p < 0.0001$). Furthermore, the addition of AGR2 to the media did not increase the number of invading vector control cells. However, AGR2 supplemented media did increase the number of invading knockdown cells relative to those cells exposed to unsupplemented media ($p < 0.05$). Additionally, those knockdown cells exposed to a higher concentration of AGR2 demonstrated higher rates of invasion (Fig. 3B). This suggests that AGR2 is a critical element of the invasion phenotype of HNSCC cells.

We have previously demonstrated that suppression of CD147 reduces in vivo tumor growth via down-regulation of oncogenic cell proliferation and reduction angiogenesis [45]. In this investigation, we used an orthotopic model to assess the effects of CD147 and AGR2 expression on the incidence of regional metastasis. Knockdown of both CD147 and AGR2 reduced primary tumor growth rate of OSC-19 xenografts and prevented primary growth of FADU xenografts. Histologic analysis of lymph nodes from OSC-19 xenografts found knockdown of CD147 or AGR2 reduced the number of positive regional lymph node and distant metastases. In addition, treatment of orthotopic OSC-19 xenografts with anti-CD147 reduced primary tumor growth rate and the incidence of bilateral regional lymph node metastasis.

To our knowledge, this is the first study to explore the association of CD147 and AGR2 with metastasis of HNSCC *in vivo*. Our findings indicate both CD147 and AGR2 play a role in tumorigenesis, coinciding with findings from previous investigations. Decreased expression and inhibition of CD147 and AGR2 reduces HNSCC cell proliferation, tumorigenesis and metastasis. In order to elucidate the utility of AGR2 and CD147 as an oncogenic biomarker in HNSCC, further investigations are required to improve our understanding of the intracellular and intercellular mechanisms at play. CD147 may be a valuable adjuvant therapeutic target and requires further exploration.

Supplementary Material

Refer to Web version on PubMed Central for supplementary material.

Acknowledgments

This study was supported jointly by grants for the National Institute of Health (R01CA142637-01 and 2T32CA091078-09). The funding source had no role in experimental design or manuscript composition.

Abbreviations

HNSCC head and neck squamous cell carcinoma

REFRENCES

1. Anderson AR. A hybrid mathematical model of solid tumour invasion: the importance of cell adhesion. Mathematical medicine and biology : a journal of the IMA. 2005; 22:163–186. [PubMed: 15781426]
2. Maekawa K, Sato H, Furukawa M, Yoshizaki T. Inhibition of cervical lymph node metastasis by marimastat (BB-2516) in an orthotopic oral squamous cell carcinoma implantation model. Clin Exp Metastasis. 2002; 19:513–518. [PubMed: 12405288]
3. Yu T, Wu Y, Helman JI, Wen Y, Wang C, Li L. CXCR4 promotes oral squamous cell carcinoma migration and invasion through inducing expression of MMP-9 and MMP-13 via the ERK signaling pathway. Mol Cancer Res. 2011; 9:161–172. [PubMed: 21205837]
4. Liu Y, Yu C, Qiu Y, Huang D, Zhou X, Zhang X, Tian Y. Downregulation of EphA2 expression suppresses the growth and metastasis in squamous-cell carcinoma of the head and neck in vitro and in vivo. J Cancer Res Clin Oncol. 2011
5. Biswas C, Zhang Y, DeCastro R, Guo H, Nakamura T, Kataoka H, Nabeshima K. The human tumor cell-derived collagenase stimulatory factor (renamed EMMPRIN) is a member of the immunoglobulin superfamily. Cancer research. 1995; 55:434–439. [PubMed: 7812975]
6. Rosenthal EL, Shreenivas S, Peters GE, Grizzle WE, Desmond R, Gladson CL. Expression of extracellular matrix metalloprotease inducer in laryngeal squamous cell carcinoma. Laryngoscope. 2003; 113:1406–1410. [PubMed: 12897567]
7. Riethdorf S, Reimers N, Assmann V, Kornfeld JW, Terracciano L, Sauter G, Pantel K. High incidence of EMMPRIN expression in human tumors. Int J Cancer. 2006; 119:1800–1810. [PubMed: 16721788]
8. Rosenthal EL, Zhang W, Talbert M, Raisch KP, Peters GE. Extracellular matrix metalloprotease inducer-expressing head and neck squamous cell carcinoma cells promote fibroblast-mediated type I collagen degradation in vitro. Mol Cancer Res. 2005; 3:195–202. [PubMed: 15831673]
9. Tang Y, Nakada MT, Kesavan P, McCabe F, Millar H, Rafferty P, Bugelski P, Yan L. Extracellular matrix metalloproteinase inducer stimulates tumor angiogenesis by elevating vascular endothelial cell growth factor and matrix metalloproteinases. Cancer Res. 2005; 65:3193–3199. [PubMed: 15833850]
10. Vigneswaran N, Beckers S, Waigel S, Mensah J, Wu J, Mo J, Fleisher KE, Bouquot J, Sacks PG, Zacharias W. Increased EMMPRIN (CD 147) expression during oral carcinogenesis. Exp Mol Pathol. 2006; 80:147–159. [PubMed: 16310185]
11. Maatta M, Tervahartiala T, Kaarniranta K, Tang Y, Yan L, Tuukkanen J, Sorsa T. Immunolocalization of EMMPRIN (CD147) in the human eye and detection of soluble form of EMMPRIN in ocular fluids. Curr Eye Res. 2006; 31:917–924. [PubMed: 17114117]
12. Bordador LC, Li X, Toole B, Chen B, Regezi J, Zardi L, Hu Y, Ramos DM. Expression of emmprin by oral squamous cell carcinoma. International journal of cancer Journal international du cancer. 2000; 85:347–352. [PubMed: 10652425]
13. Chen Z, Mi L, Xu J, Yu J, Wang X, Jiang J, Xing J, Shang P, Qian A, Li Y, Shaw PX, Wang J, Duan S, Ding J, Fan C, Zhang Y, Yang Y, Yu X, Feng Q, Li B, Yao X, Zhang Z, Li L, Xue X, Zhu P. Function of HAb18G/CD147 in invasion of host cells by severe acute respiratory syndrome coronavirus. J Infect Dis. 2005; 191:755–760. [PubMed: 15688292]

14. Yang JM, Xu Z, Wu H, Zhu H, Wu X, Hait WN. Overexpression of extracellular matrix metalloproteinase inducer in multidrug resistant cancer cells. Molecular cancer research : MCR. 2003; 1:420–427. [PubMed: 12692261]
15. Kuang YH, Chen X, Su J, Wu LS, Li J, Chang J, Qiu Y, Chen ZS, Kanekura T. Proteome analysis of multidrug resistance of human oral squamous carcinoma cells using CD147 silencing. Journal of proteome research. 2008; 7:4784–4791. [PubMed: 18816083]
16. Huang C, Sun Z, Sun Y, Chen X, Zhu X, Fan C, Liu B, Zhao Y, Zhang W. Association of increased ligand cyclophilin A and receptor CD147 with hypoxia, angiogenesis, metastasis and prognosis of tongue squamous cell carcinoma. Histopathology. 2012
17. Huang Z, Huang H, Li H, Chen W, Pan C. EMMPRIN expression in tongue squamous cell carcinoma. J Oral Pathol Med. 2009; 38:518–523. [PubMed: 19473445]
18. Cheng MF, Tzao C, Tsai WC, Lee WH, Chen A, Chiang H, Sheu LF, Jin JS. Expression of EMMPRIN and matriptase in esophageal squamous cell carcinoma: correlation with clinicopathological parameters. Dis Esophagus. 2006; 19:482–486. [PubMed: 17069593]
19. Zheng HC, Takahashi H, Murai Y, Cui ZG, Nomoto K, Miwa S, Tsuneyama K, Takano Y. Upregulated EMMPRIN/CD147 might contribute to growth and angiogenesis of gastric carcinoma: a good marker for local invasion and prognosis. Br J Cancer. 2006; 95:1371–1378. [PubMed: 17088917]
20. Zheng HC, Wang W, Xu XY, Xia P, Yu M, Sugiyama T, Takano Y. Up-regulated EMMPRIN/CD147 protein expression might play a role in colorectal carcinogenesis and its subsequent progression without an alteration of its glycosylation and mRNA level. J Cancer Res Clin Oncol. 2011; 137:585–596. [PubMed: 20514493]
21. Rosenthal EL, Shreenivas S, Peters GE, Grizzle WE, Desmond R, Gladson CL. Expression of extracellular matrix metalloprotease inducer in laryngeal squamous cell carcinoma. Laryngoscope. 2003; 113:1406–1410. [PubMed: 12897567]
22. Wang Z, Hao Y, Lowe AW. The adenocarcinoma-associated antigen, AGR2, promotes tumor growth, cell migration, and cellular transformation. Cancer research. 2008; 68:492–497. [PubMed: 18199544]
23. Maresh EL, Mah V, Alavi M, Horvath S, Bagryanova L, Liebeskind ES, Knutzen LA, Zhou Y, Chia D, Liu AY, Goodglick L. Differential expression of anterior gradient gene AGR2 in prostate cancer. BMC Cancer. 2010; 10:680. [PubMed: 21144054]
24. Thompson DA, Weigel RJ. hAG-2, the human homologue of the Xenopus laevis cement gland gene XAG-2, is coexpressed with estrogen receptor in breast cancer cell lines. Biochem Biophys Res Commun. 1998; 251:111–116. [PubMed: 9790916]
25. Fritzsche FR, Dahl E, Pahl S, Burkhardt M, Luo J, Mayordomo E, Gansukh T, Dankof A, Knuechel R, Denkert C, Winzer KJ, Dietel M, Kristiansen G. Prognostic relevance of AGR2 expression in breast cancer. Clin Cancer Res. 2006; 12:1728–1734. [PubMed: 16551856]
26. Zhang JS, Gong A, Cheville JC, Smith DI, Young CY. AGR2, an androgen-inducible secretory protein overexpressed in prostate cancer. Genes Chromosomes Cancer. 2005; 43:249–259. [PubMed: 15834940]
27. Zhang Y, Forootan SS, Liu D, Barraclough R, Foster CS, Rudland PS, Ke Y. Increased expression of anterior gradient-2 is significantly associated with poor survival of prostate cancer patients. Prostate Cancer Prostatic Dis. 2007; 10:293–300. [PubMed: 17457305]
28. Riener MO, Pilarsky C, Gerhardt J, Grutzmann R, Fritzsche FR, Bahra M, Weichert W, Kristiansen G. Prognostic significance of AGR2 in pancreatic ductal adenocarcinoma. Histol Histopathol. 2009; 24:1121–1128. [PubMed: 19609859]
29. Fritzsche FR, Dahl E, Dankof A, Burkhardt M, Pahl S, Petersen I, Dietel M, Kristiansen G. Expression of AGR2 in non small cell lung cancer. Histol Histopathol. 2007; 22:703–708. [PubMed: 17455144]
30. Park K, Chung YJ, So H, Kim K, Park J, Oh M, Jo M, Choi K, Lee EJ, Choi YL, Song SY, Bae DS, Kim BG, Lee JH. AGR2, a mucinous ovarian cancer marker, promotes cell proliferation and migration. Exp Mol Med. 2011; 43:91–100. [PubMed: 21200134]

31. Liu D, Rudland PS, Sibson DR, Platt-Higgins A, Barraclough R. Human homologue of cement gland protein, a novel metastasis inducer associated with breast carcinomas. Cancer Res. 2005; 65:3796–3805. [PubMed: 15867376]
32. Zweitzig DR, Smirnov DA, Connelly MC, Terstappen LW, O'Hara SM, Moran E. Physiological stress induces the metastasis marker AGR2 in breast cancer cells. Molecular and cellular biochemistry. 2007; 306:255–260. [PubMed: 17694278]
33. Park SW, Zhen G, Verhaeghe C, Nakagami Y, Nguyenvu LT, Barczak AJ, Killeen N, Erle DJ. The protein disulfide isomerase AGR2 is essential for production of intestinal mucus. Proc Natl Acad Sci U S A. 2009; 106:6950–6955. [PubMed: 19359471]
34. Zhang Y, Ali TZ, Zhou H, D'Souza DR, Lu Y, Jaffe J, Liu Z, Passaniti A, Hamburger AW. ErbB3 binding protein 1 represses metastasis-promoting gene anterior gradient protein 2 in prostate cancer. Cancer Res. 2010; 70:240–248. [PubMed: 20048076]
35. Liu Z, Hartman YE, Warram JM, Knowles JA, Sweeny L, Zhou T, Rosenthal EL. Fibroblast growth factor receptor mediates fibroblast-dependent growth in EMMPRIN-depleted head and neck cancer tumor cells. Mol Cancer Res. 2011; 9:1008–1017. [PubMed: 21665938]
36. Dean NR, Newman JR, Helman EE, Zhang W, Safavy S, Weeks DM, Cunningham M, Snyder LA, Tang Y, Yan L, McNally LR, Buchsbaum DJ, Rosenthal EL. Anti-EMMPRIN monoclonal antibody as a novel agent for therapy of head and neck cancer. Clin Cancer Res. 2009; 15:4058–4065. [PubMed: 19509148]
37. Gleysteen JP, Newman JR, Chhieng D, Frost A, Zinn KR, Rosenthal EL. Fluorescent labeled anti-EGFR antibody for identification of regional and distant metastasis in a preclinical xenograft model. Head Neck. 2008; 30:782–789. [PubMed: 18228526]
38. Kulbersh BD, Duncan RD, Magnuson JS, Skipper JB, Zinn K, Rosenthal EL. Sensitivity and specificity of fluorescent immunoguided neoplasm detection in head and neck cancer xenografts. Arch Otolaryngol Head Neck Surg. 2007; 133:511–515. [PubMed: 17520766]
39. Rosenthal EL, Kulbersh BD, King T, Chaudhuri TR, Zinn KR. Use of fluorescent labeled anti-epidermal growth factor receptor antibody to image head and neck squamous cell carcinoma xenografts. Mol Cancer Ther. 2007; 6:1230–1238. [PubMed: 17431103]
40. Gleysteen JP, Newman JR, Chhieng D, Frost A, Zinn KR, Rosenthal EL. Fluorescent labeled anti-EGFR antibody for identification of regional and distant metastasis in a preclinical xenograft model. Head Neck. 2008; 30:782–789. [PubMed: 18228526]
41. Erdem NF, Carlson ER, Gerard DA, Ichiki AT. Characterization of 3 oral squamous cell carcinoma cell lines with different invasion and/or metastatic potentials. J Oral Maxillofac Surg. 2007; 65:1725–1733. [PubMed: 17719389]
42. Marieb EA, Zoltan-Jones A, Li R, Misra S, Ghatak S, Cao J, Zucker S, Toole BP. Emmprin promotes anchorage-independent growth in human mammary carcinoma cells by stimulating hyaluronan production. Cancer Res. 2004; 64:1229–1232. [PubMed: 14983875]
43. Quemener C, Gabison EE, Naimi B, Lescaille G, Bougatef F, Podgorniak MP, Labarchede G, Lebbe C, Calvo F, Menashi S, Mourah S. Extracellular matrix metalloproteinase inducer up-regulates the urokinase-type plasminogen activator system promoting tumor cell invasion. Cancer Res. 2007; 67:9–15. [PubMed: 17210677]
44. Yan L, Zucker S, Toole BP. Roles of the multifunctional glycoprotein, emmprin (basigin; CD147), in tumour progression. Thromb Haemost. 2005; 93:199–204. [PubMed: 15711733]
45. Newman JR, Bohannon IA, Zhang W, Skipper JB, Grizzle WE, Rosenthal EL. Modulation of tumor cell growth in vivo by extracellular matrix metalloprotease inducer. Archives of otolaryngology--head & neck surgery. 2008; 134:1218–1224. [PubMed: 19015455]
46. Tsukifuji R, Tagawa K, Hatamochi A, Shinkai H. Expression of matrix metalloproteinase-1, -2 and -3 in squamous cell carcinoma and actinic keratosis. Br J Cancer. 1999; 80:1087–1091. [PubMed: 10362121]
47. Sutinen M, Kainulainen T, Hurskainen T, Vesterlund E, Alexander JP, Overall CM, Sorsa T, Salo T. Expression of matrix metalloproteinases (MMP-1 and -2) and their inhibitors (TIMP-1, -2 and -3) in oral lichen planus, dysplasia, squamous cell carcinoma and lymph node metastasis. Br J Cancer. 1998; 77:2239–2245. [PubMed: 9649139]

Highlights

- We investigated AGR2 in head and neck squamous cell carcinoma for the first time.
- We explored the relationship between AGR2 and CD147 for the first time.
- AGR2 and CD147 appear to co-localize in head and squamous cell carcinoma samples.
- Knockdown of both AGR2 and CD147 reduced migration and invasion in vitro.
- Knockdown of both AGR2 and CD147 decreased metastasis in vivo.

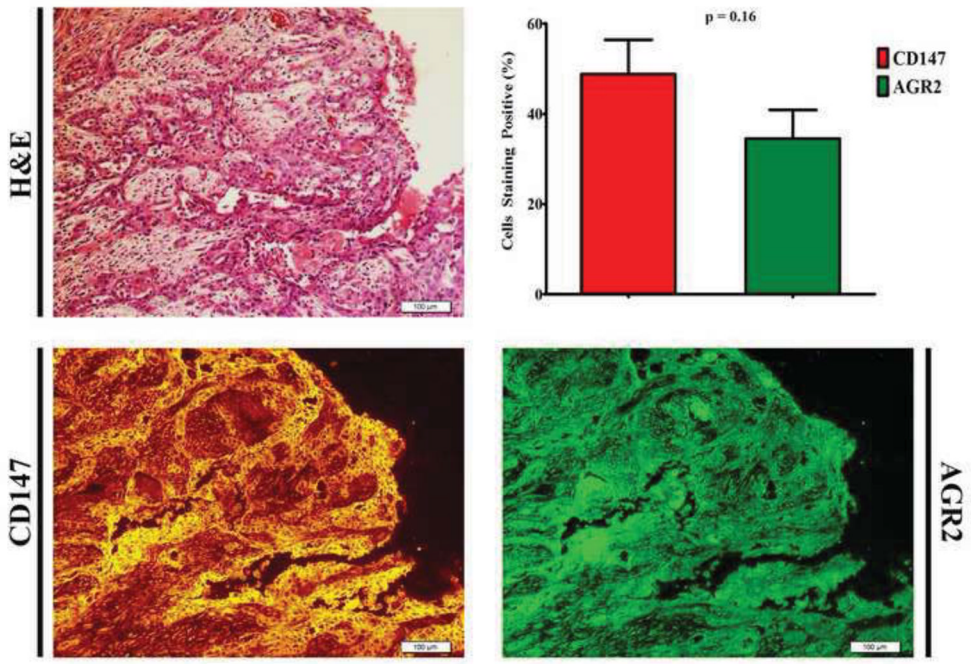

Fig. 1.

The expression patterns of CD147 and AGR2 in HNSCC were evaluated by immunofluorescence analysis of oral cavity squamous cell carcinoma specimens (n=20). Approximately half of the oncogenic cells demonstrated CD147 expression while close to a third demonstrated AGR2 immunoreactivity. CD147 expression was primarily membranous, while AGR2 immunoreactivity was predominately cytoplasmic.

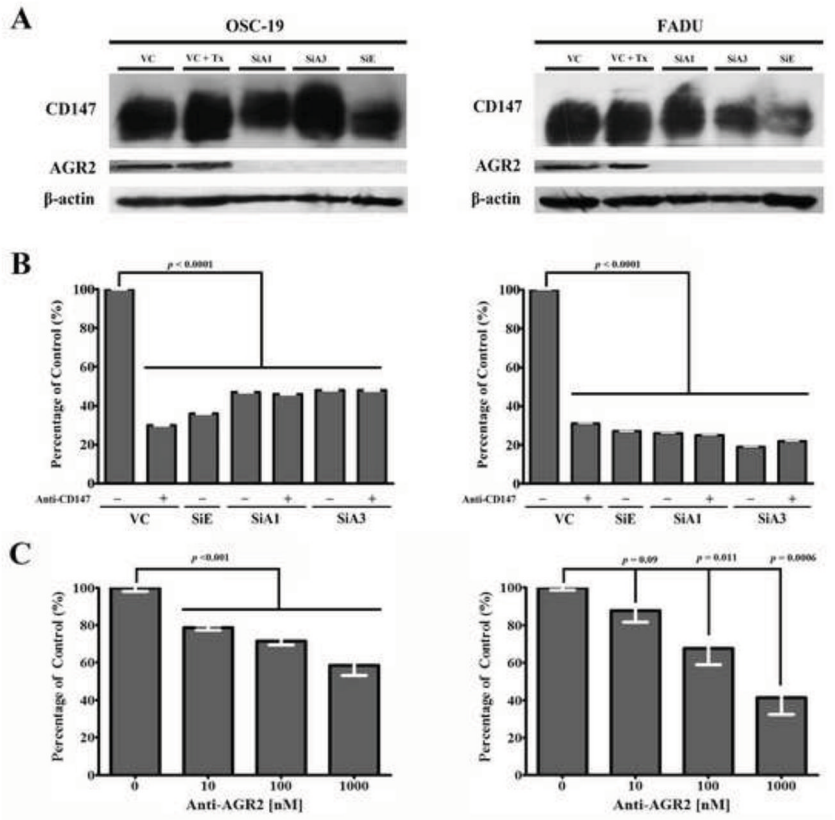

Fig. 2.

Western blot analysis (A) of protein expression levels verified knockdown of CD147 expression by OSC-19/siE and FADU/siE and knockdown of AGR2 expression by OSC-19/siA and FADU/siA cell lines relative to vector control (VC). Additionally, knockdown of CD147 correlated with an absence of AGR2 expression. Treatment of vector control cells with anti-CD147 (Tx) had no effect on CD147 or AGR2 expression levels. Proliferation of OSC-19 and FADU vector control and knockdown (siE, siA1, siA3) cell lines (B) was assessed following 48 h ± anti-CD147 (200 μg/mL). Relative to vector control, a reduction of CD147 or AGR2 expression resulted in a significant decrease in cell proliferation. There was a reduction in proliferation of OSC-19/VC and FADU/VC cell lines following treatment with anti-AGR2 (C). Columns, mean for triplicate; bars, SE.

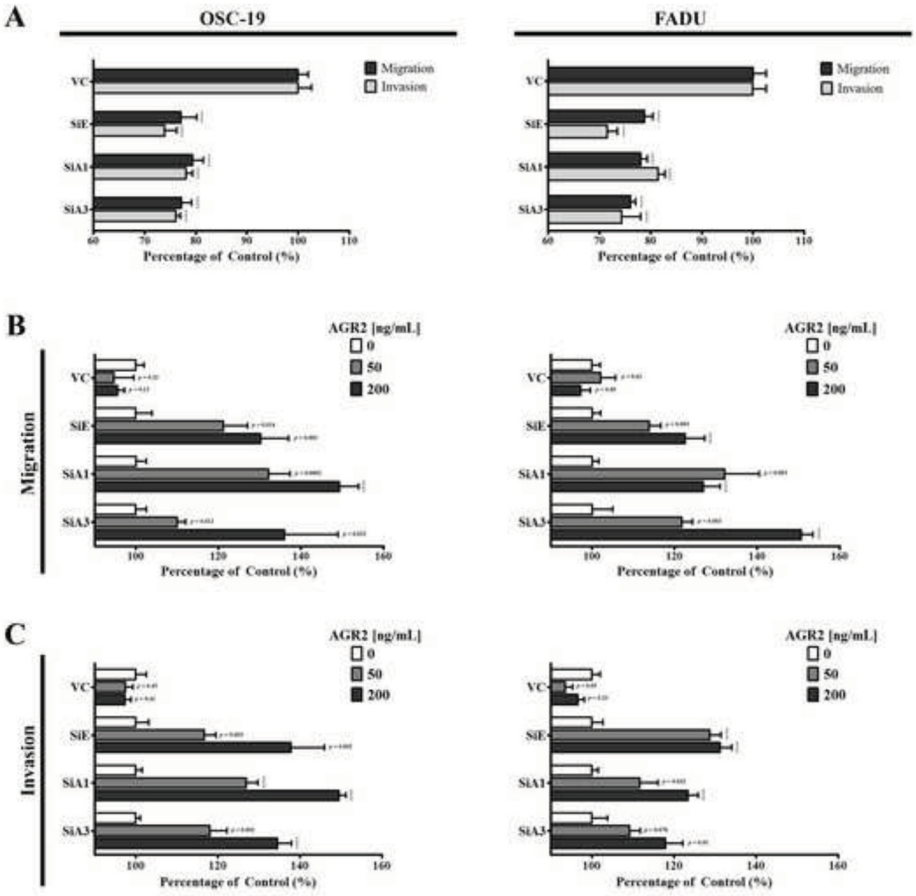

Fig. 3.

Migration and invasion were evaluated by a transwell chamber system. Reduction in CD147 or AGR2 expression significantly decreased both migration and invasion of OSC-19 and FADU knockdown cells compared to vector control (A). Addition of AGR2 to the media did not affect migration (B) or invasion (C) of OSC-19/VC or FADU/VC cell lines. However, supplementing the media with either 50 or 200 ng/mL of AGR2 significantly increased both migration (B) and invasion (C) of both the OSC-19 and FADU knockdown CD147 and AGR2 cell lines. Statistical significance by unpaired t-test, ****p<0.0001. Columns, mean for triplicate; bars, SE.

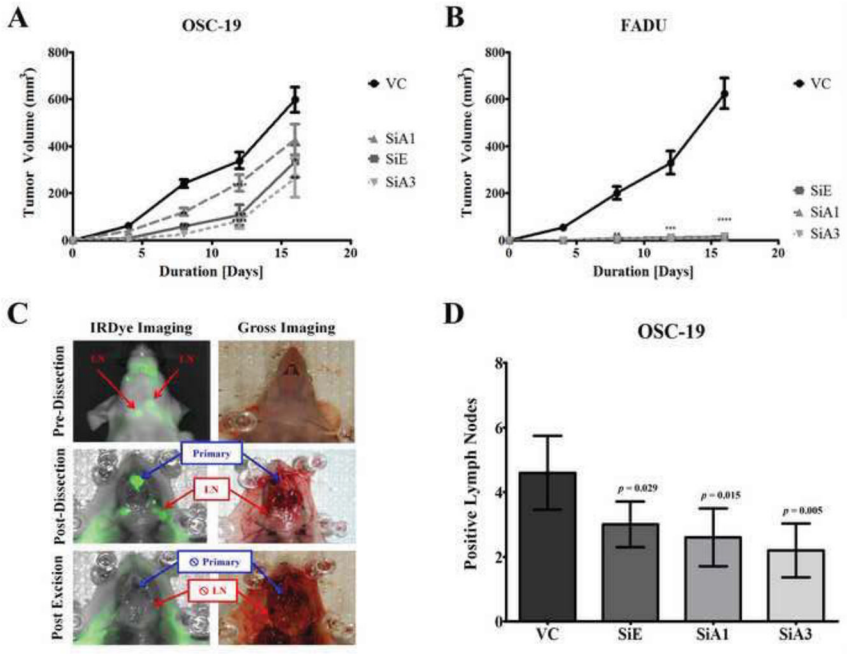

Fig. 4.

The role of CD147 and AGR2 in primary tumor growth and cervical lymph node metastasis was assessed using an oral cavity orthotopic tongue model. OSC-19 (A) or FADU (B) vector control or knockdown cells lines were implanted in the proximal tongue of athymic nude mice (n=5/group). The knockdown cell lines demonstrated a reduction in tumor growth rate which maintained for the duration of the study. The OSC-19/VC had significantly larger tumor volumes (597.4 mm^3) compared to OSC-19/siE (336.0 mm^3), OSC-19/siA1 (428.4 mm^3) or OSC-19/siA3 (265.8 mm^3) (A). The FADU/VC xenografts had significantly larger tumor volumes (624.2 mm^3) compared to FADU/siE (16.3 mm^3), FADU/siA1 (10.1 mm^3) or FADU/siA3 (12.6 mm^3) (B). Targeted fluorescence imaging assisted in localization of primary disease and lymph node metastasis (C). Microscopically, regional lymph node metastases were detected in all OSC-19 xenografts. However, there was a significant difference in the number of positive lymph nodes of the knockdown cells relative to vector control (D). Statistical significance by unpaired t-test, *p<0.05, **p<0.01, ****p<0.001, ****p<0.0001. Columns or marker, mean for triplicate; bars, SE.

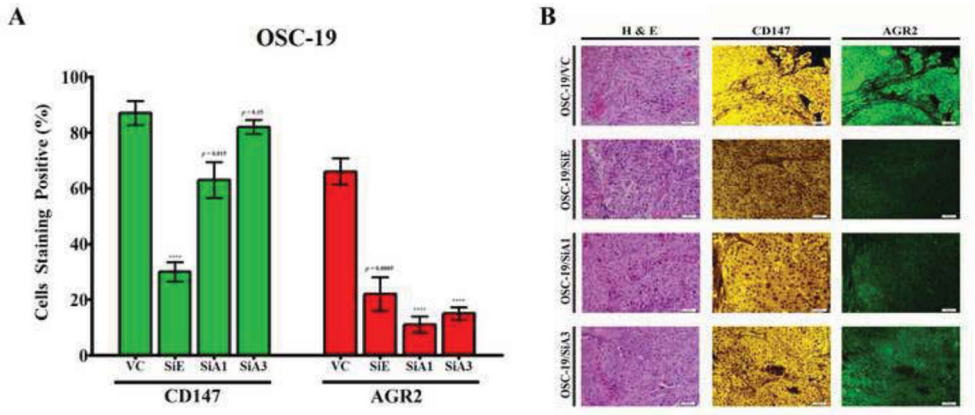

Fig. 5.

Primary lesions underwent further histologic analyses for CD147 and AGR2 expression. Relative to OSC-19/VC (87%), there was a significant reduction in CD147 immunoreactivity in OSC-19/siE (30%) and OSC-19/siA1 (63%) xenografts. Similarly, there was a significant reduction in AGR2 immunoreactivity in OSC-19/siE (22%), OSC-19/siA1 (11 %) and OSC-19/siA1 (15%) xenografts relative to OSC-19/VC (66%). Columns, mean for triplicate; bars, SE.

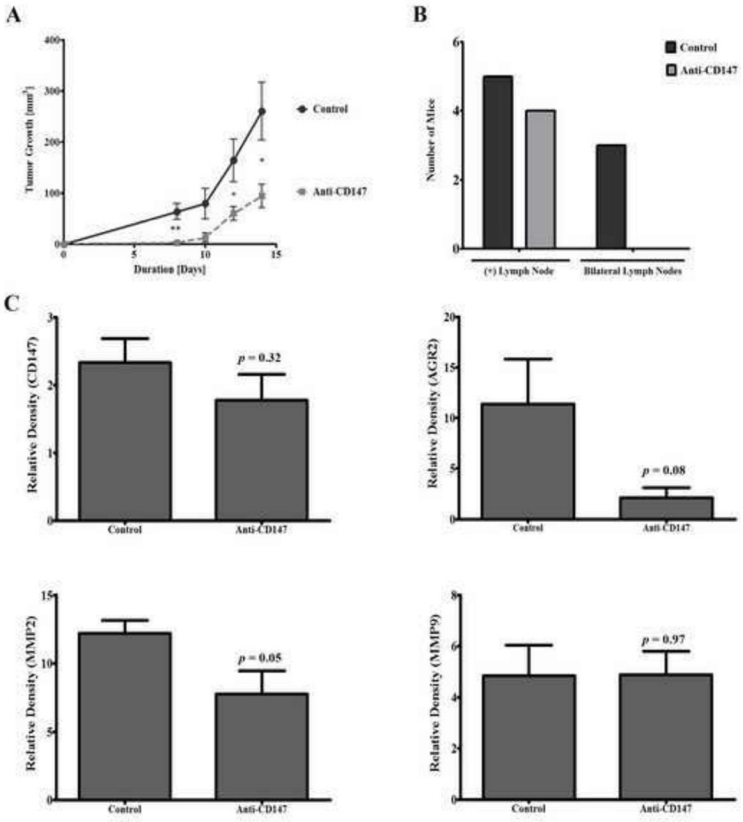

Fig. 6.

Orthotopic OSC-19 xenografts were divided into two cohorts: control and anti-CD147 treatment. Anti-CD147 treatment (200 μg i.p./triweekly) was begun on the day of tumor cell implantation. By day 8, there was a significant reduction in tumor growth rate (A). The incidence of positive lymph nodes was similar between the two cohorts (B). However, none of the mice in treatment cohort had evidence of bilateral lymph node (BLN) metastasis while 60% (n=3) had positive BLN in the control group (B). Lysates of primary lesions were prepared for western blot and zymogram analysis. There was a trend toward decreased CD147 (C) and AGR2 (B) expression in the treatment group. Furthermore, there was a significant decrease in MMP2 expression in the treatment cohort (E). Statistical significance by unpaired t-test, $*p<0.05$, $**p<0.01$. Columns or marker, mean for triplicate; bars, SE.